

HEALTH AND MEDICINE

The essential role of the transporter ABCG2 in the pathophysiology of erythropoietic protoporphyria

Pengcheng Wang^{1*}, Madhav Sachar^{1*}, Jie Lu¹, Amina I. Shehu¹, Junjie Zhu¹, Jing Chen¹, Ke Liu¹, Karl E. Anderson², Wen Xie¹, Frank J. Gonzalez³, Curtis D. Klaassen⁴, Xiaochao Ma^{1†}

Erythropoietic protoporphyria (EPP) is an inherited disease caused by loss-of-function mutations of ferrochelatase, an enzyme in the heme biosynthesis pathway that converts protoporphyrin IX (PPIX) into heme. PPIX accumulation in patients with EPP leads to phototoxicity and hepatotoxicity, and there is no cure. Here, we demonstrated that the PPIX efflux transporter ABCG2 (also called BCRP) determines EPP-associated phototoxicity and hepatotoxicity. We found that ABCG2 deficiency decreases PPIX distribution to the skin and therefore prevents EPP-associated phototoxicity. We also found that ABCG2 deficiency protects against EPP-associated hepatotoxicity by modulating PPIX distribution, metabolism, and excretion. In summary, our work has uncovered an essential role of ABCG2 in the pathophysiology of EPP, which suggests the potential for novel strategies in the development of therapy for EPP.

INTRODUCTION

The porphyrias are a group of metabolic disorders of the heme biosynthesis pathway (1). Erythropoietic protoporphyria (EPP) is the third most common type of porphyria and the most common porphyria in childhood (2). EPP is caused by loss-of-function mutations of ferrochelatase (FECH), the last enzyme in the heme biosynthesis pathway that incorporates Fe²⁺ with protoporphyrin IX (PPIX) to form heme (3, 4). Because of FECH deficiency, PPIX substantially accumulates in patients with EPP, mainly in red blood cells (RBCs), plasma, skin, and the liver. In addition to EPP, PPIX accumulation also occurs in X-linked protoporphyria (XLP), another type of porphyria caused by gain-of-function mutations of δ -aminolevulinic synthase 2 (ALAS2) (5, 6), the rate-limiting enzyme in the heme biosynthesis pathway. Furthermore, many clinically used drugs and environmental toxins, including rifampicin (RIF), isoniazid (INH), diethoxycarbonyl-1,4-dihydrocollidine (DDC), and griseofulvin (GSF), can cause PPIX accumulation in the liver through the induction of ALAS1 and/or inhibition of FECH (7–13).

Accumulation of PPIX in the skin leads to phototoxicity in patients with EPP. PPIX is a tetrapyrrole rich in electrons. When patients with EPP are exposed to light, PPIX gets excited and releases its energy to oxygen that can produce free radicals and result in skin damage (5, 14). Symptoms of skin reactions include purpura, erythema, edema, and a burning sensation in the skin (5, 14, 15). Therefore, patients with EPP must avoid light by decreasing outdoor activities and/or using protective clothing, which negatively affect their social and work activities and overall quality of life (14, 15). Current therapies for phototoxicity in patients with EPP focus on decreasing the permeation of light into the skin and/or managing skin lesions

resulting from light-excited PPIX (5, 14, 15). Beta-carotene has been used in patients with EPP because of its antioxidant effects, as well as its ability to increase skin pigmentation and reduce the penetration of light into the skin, but is marginally effective (5, 16). Afamelanotide reduces the skin symptoms in patients with EPP by increasing melanin synthesis and decreasing the penetration of light into the skin (17). Despite these treatment options, no therapy currently addresses the underlying cause of phototoxicity in EPP, which is the accumulation of PPIX in the skin.

In addition to the skin, the liver is another target organ of PPIX toxicity in EPP, and its severity is affected by the polymorphisms of genes regulating porphyrin homeostasis (18). The liver is responsible for PPIX elimination from the body through the hepatobiliary system. Because PPIX is highly hydrophobic, excessive PPIX in bile will precipitate and lead to bile duct blockage and cholestatic liver injury (5, 15, 19). Multiple pharmacological approaches have been attempted to manage EPP-associated liver injury in the clinic, but none have produced satisfactory outcomes (19). Liver transplant is effective, but the recurrence of EPP-associated liver injury is common because the liver transplant cannot restore FECH function in the bone marrow and cannot prevent PPIX accumulation in the liver (20). Therefore, novel strategies are needed for the management of EPP-associated liver injury.

In EPP, PPIX is predominantly produced in the bone marrow and delivered to other organs, including the skin and liver, through the circulatory system by RBCs and plasma. Efflux of PPIX from RBCs into plasma is dependent on the transporter ABCG2 (21), and exposure to light promotes PPIX efflux (22). These data led us to hypothesize that suppression of ABCG2 will decrease the disposition of PPIX to the skin and mitigate phototoxicity in EPP. In addition, a prior report showed that retention of PPIX in hepatocytes and Kupffer cells, but not in the biliary system, attenuates EPP-associated hepatotoxicity (23). ABCG2 is expressed in hepatocytes and is responsible for PPIX efflux from hepatocytes into the biliary system (24). Therefore, we also hypothesized that suppression of ABCG2 will decrease the amount of PPIX in the biliary system and attenuate PPIX-mediated bile duct blockage and cholestatic liver injury.

¹Center for Pharmacogenetics, Department of Pharmaceutical Sciences, School of Pharmacy, University of Pittsburgh, Pittsburgh, PA 15261, USA. ²Porphyria Laboratory and Center, Departments of Preventive Medicine and Community Health, and Internal Medicine, University of Texas Medical Branch, Galveston, TX 77555, USA. ³Laboratory of Metabolism, Center for Cancer Research, National Cancer Institute, NIH, Bethesda, MD 20892, USA. ⁴Department of Pharmacology, Toxicology and Therapeutics, University of Kansas Medical Center, Kansas City, KS 66160, USA.

*These authors contributed equally to this work.

†Corresponding author. Email: mxiaocha@pitt.edu

An EPP mouse model was developed by a loss-of-function mutation of FECH (Fech-mut) (25, 26). To test our hypotheses, we generated an EPP mouse model with ABCG2 deficiency (Fech-mut/*Abcg2*-null). We found that ABCG2 deficiency abolished both phototoxicity and hepatotoxicity in EPP mice. We also found that *Abcg2*-null mice failed to develop PPIX accumulation and hepatotoxicity when these mice were challenged with liver-specific porphyrinogenic chemicals. Our metabolomic analysis further revealed that ABCG2 deficiency protects against PPIX-mediated phototoxicity and hepatotoxicity by modulating PPIX distribution, metabolism, and excretion.

RESULTS

ABCG2 deficiency protects against EPP-associated phototoxicity

Fech-mut/*Abcg2*-null mice have a loss-of-function mutation of FECH and are deficient in ABCG2 (Fig. 1A). When Fech-mut/*Abcg2*-null and Fech-mut mice were exposed to light with the excitation wavelength of PPIX (395 to 410 nm), Fech-mut mice developed severe skin lesions, but these phenotypes were absent in Fech-mut/*Abcg2*-null mice (Fig. 1, B to F, and fig. S1, A to D). In addition, no skin injury was observed in Fech-mut/*Abcg2*-null mice exposed to long-wavelength light (630 nm) (fig. S2). Furthermore, oxidative stress and inflammation were observed in the skin of Fech-mut mice after light exposure (395 to 410 nm), but not in Fech-mut/*Abcg2*-null mice (fig. S1, E to G). These data indicate that ABCG2 is the key mediator of EPP-associated phototoxicity. We next analyzed PPIX levels in RBCs, serum, and the skin of EPP mouse models. We found that ABCG2 deficiency significantly increased PPIX levels in RBCs but decreased PPIX levels in serum and skin (Fig. 1, G to I), suggesting that dysfunction of ABCG2 blocks PPIX efflux from RBCs into plasma and therefore decreases PPIX distribution to the skin and attenuates PPIX-mediated phototoxicity (Fig. 1J).

ABCG2 deficiency protects against EPP-associated hepatotoxicity

As expected, liver damage occurred in Fech-mut mice (25, 26), but it was abolished in Fech-mut/*Abcg2*-null mice (Fig. 2). Compared to Fech-mut mice, the serum biomarkers of liver damage were significantly decreased in Fech-mut/*Abcg2*-null mice (Fig. 2, A to D). The decrease of serum alkaline phosphatase (ALP) activity in Fech-mut/*Abcg2*-null mice (Fig. 2C) indicates attenuation of cholestatic liver damage. PPIX levels in the liver of Fech-mut/*Abcg2*-null mice were significantly decreased (Fig. 2E and fig. S3), and PPIX-mediated bile duct blockage and bile plugs were not observed in the liver of Fech-mut/*Abcg2*-null mice (Fig. 2, F to I and fig. S3). Liver fibrosis is a critical step in the progression of EPP-associated liver damage (5, 19). We observed liver fibrosis in Fech-mut mice, but it was abrogated in Fech-mut/*Abcg2*-null mice (fig. S4). These data indicate that ABCG2 plays an essential role in the development of EPP-associated liver injury.

ABCG2 deficiency protects against chemically induced PPIX accumulation and hepatotoxicity

To further determine the role of ABCG2 in PPIX-mediated liver injury, wild-type (WT) and *Abcg2*-null mice were challenged with DDC or GSF, two model chemicals that cause hepatic PPIX accu-

mulation and hepatotoxicity (12, 13). While DDC and GSF caused liver damage, PPIX accumulation, and bile plugs in WT mice, these effects were very minor or absent in *Abcg2*-null mice (Fig. 3 and fig. S5). In addition to DDC and GSF, our previous study found that cotreatment with RIF and INH resulted in hepatic PPIX accumulation and hepatotoxicity through the human pregnane X receptor (hPXR)-mediated pathway (7). To determine the role of ABCG2 in RIF and INH-induced PPIX accumulation and hepatotoxicity, an hPXR mouse model deficient in ABCG2 (hPXR/*Abcg2*-null) was generated (Fig. 4A). Hepatotoxicity along with PPIX accumulation and bile plugs were observed in hPXR mice cotreated with RIF and INH, but these phenotypes were abolished in hPXR/*Abcg2*-null mice (Fig. 4, B to F). These data further confirmed that PPIX-mediated liver injury is dependent on ABCG2.

ABCG2 deficiency modulates PPIX distribution, metabolism, and excretion

To understand the mechanisms by which deficiency of ABCG2 abolishes PPIX accumulation and hepatotoxicity, metabolomic analyses of liver and bile samples (Fig. 5, A to C) were conducted in WT and *Abcg2*-null mice treated with deuterium-labeled aminolevulinic acid (D_2 -ALA), a precursor of PPIX (15). As expected, D_{16} -PPIX was identified as a downstream metabolite of D_2 -ALA. Consistent with the notion that PPIX is an ABCG2 substrate (24), the excretion of D_{16} -PPIX to bile was significantly decreased in *Abcg2*-null mice when compared to WT mice (Fig. 5D), suggesting that deficiency of ABCG2 can directly decrease PPIX levels in the biliary system and thus prevent PPIX-mediated bile duct blockage. A small amount of D_{16} -PPIX was detected in the bile of *Abcg2*-null mice (Fig. 5D), indicating that transporter(s) other than ABCG2 might be involved in PPIX efflux, although they are less effective. We observed the compensatory changes of efflux transporters in the liver of ABCG2-deficient mice (fig. S6). Future studies will determine which specific transporter serves as an alternative pathway for PPIX efflux in the absence of ABCG2.

Metabolomic analysis also led to the discovery of D_{16} -protoporphyrin-1-*O*-acyl-glucuronide (D_{16} -PPIX-glu) as a conjugated metabolite of D_{16} -PPIX. The structure of D_{16} -PPIX-glu was verified by comparing it to the synthesized chemical standard of PPIX-glu (fig. S7). D_{16} -PPIX-glu levels in the liver and bile of *Abcg2*-null mice were significantly increased when compared to WT mice (Fig. 5, E and F). PPIX-glu was also identified in the bile of Fech-mut/*Abcg2*-null mice (Fig. 5G). In addition to PPIX-glu, two known conjugated metabolites of PPIX, protoporphyrin-1-*O*-acyl- β -glucoside and protoporphyrin-1-*O*-acyl- β -xyloside (27), were identified in the bile of Fech-mut/*Abcg2*-null mice (Fig. 5G). Overall, the conjugated metabolites of PPIX were substantially increased in the bile of Fech-mut/*Abcg2*-null mice when compared to Fech-mut mice (Fig. 5H). The conjugated metabolites are considered detoxified metabolites because they are more hydrophilic and more readily excreted than the parent compound (28). Therefore, our data suggest that deficiency of ABCG2 in hepatocytes increases the conjugation pathways of PPIX and facilitates PPIX excretion in the EPP condition (Fig. 5I). Furthermore, ABCG2 deficiency in RBCs decreased PPIX levels in plasma (Fig. 1H), which, in turn, decreased PPIX uptake by hepatocytes and decreased PPIX levels in the biliary system consequently attenuating PPIX-mediated bile duct blockage (Fig. 5I).

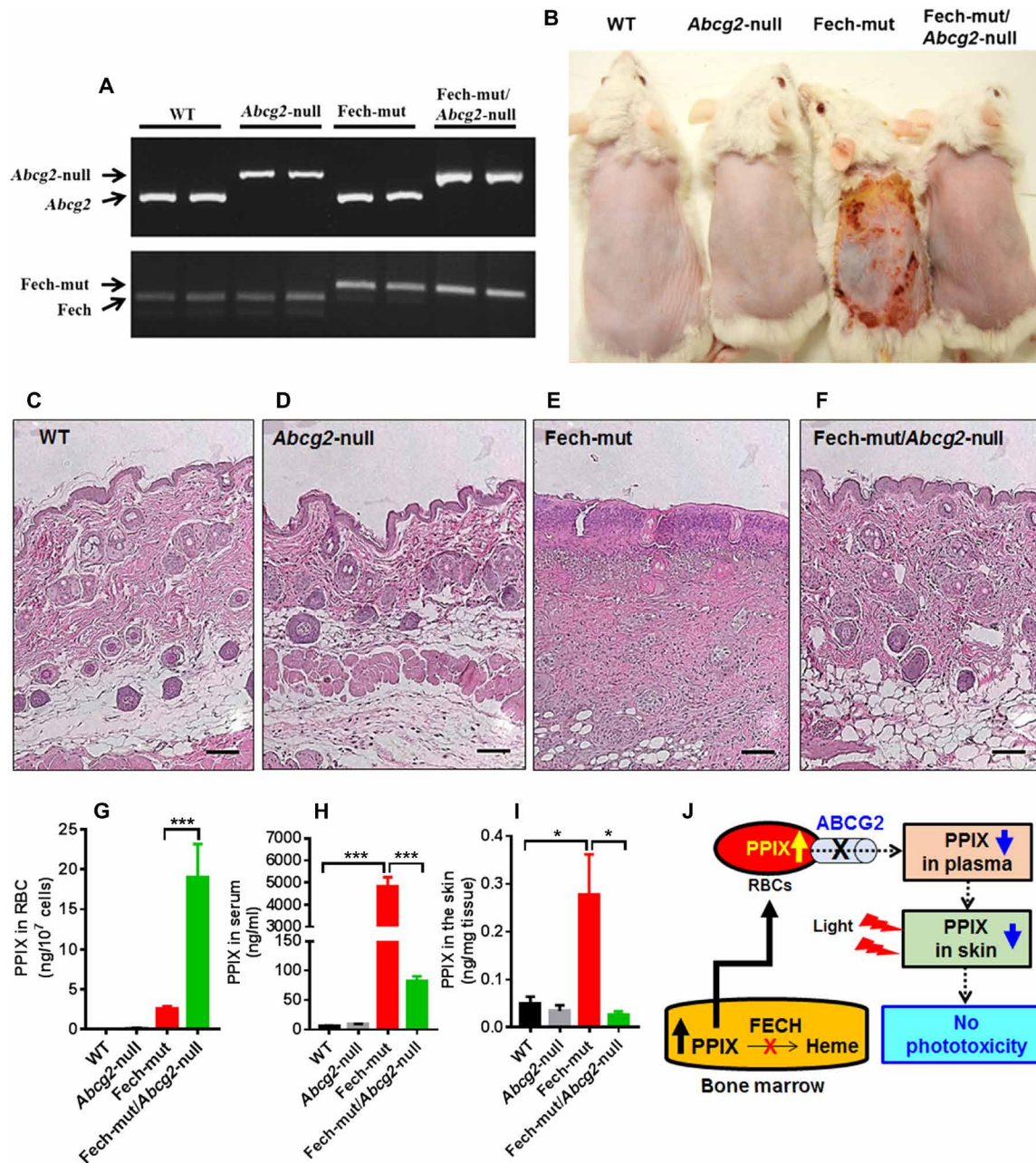


Fig. 1. Essential role of ABCG2 in EPP-associated phototoxicity. (A) Genotyping results of WT, *Abcg2*-null, *Fech*-mut, and *Fech*-mut/*Abcg2*-null mice. *Fech*-mut/*Abcg2*-null mice are deficient in both *Fech* and *Abcg2*. (B) Gross appearance of mice after light exposure. The back skin of mice was shaved and exposed to UV light (395 to 410 nm) for 30 min each day for 5 days. (C to F) Histologic sections of mouse skin after exposure to UV light, hematoxylin and eosin (H&E) staining. Scale bars, 40 μ m. (G) PPIX levels in RBCs. (H) PPIX levels in serum. (I) PPIX levels in the skin of mice after exposure to UV light. PPIX was analyzed by UPLC-QTOFMS. All data are expressed as means \pm SEM ($n = 4$ per group). * $P < 0.05$, *** $P < 0.001$, one-way ANOVA. (J) A schematic showing that deficiency of ABCG2 decreases PPIX distribution to the skin and abrogates PPIX-mediated phototoxicity in EPP. (Photo credit: Pengcheng Wang, University of Pittsburgh.)

DISCUSSION

Phototoxicity is the most common symptom in patients with EPP (2, 29, 30). Our work demonstrated that the phototoxicity in EPP is dependent on ABCG2. Compared to *Fech*-mut mice, PPIX levels were substantially increased in RBCs but decreased in serum and the skin of *Fech*-mut/*Abcg2*-null mice. Concordantly, the phototoxicity observed in *Fech*-mut mice was abolished in *Fech*-mut/*Abcg2*-null mice. These data indicate that ABCG2 in RBCs drives

phototoxicity in EPP by increasing PPIX distribution to the skin (Fig. 6A). In addition, ABCG2-dependent delivery of PPIX to the biliary system causes bile duct blockage, which further increases PPIX accumulation in the body and, in turn, potentiates phototoxicity (Fig. 6A). Our data suggest that inhibition of ABCG2 can be used as a novel strategy for the management of EPP-associated phototoxicity, as ABCG2 deficiency will decrease the accumulation of PPIX in the skin and prevent phototoxicity (Fig. 6B).

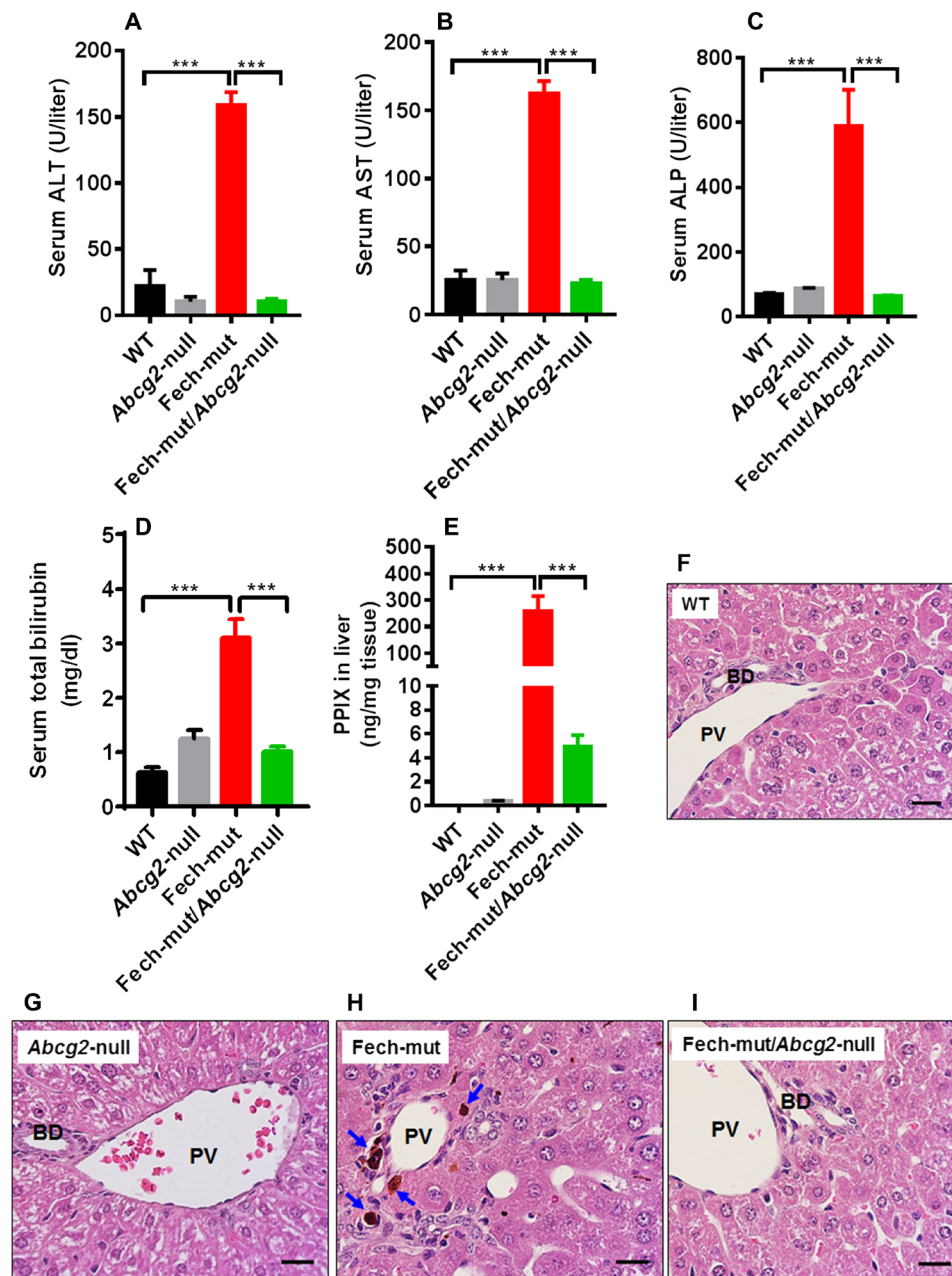


Fig. 2. EPP-associated hepatotoxicity is dependent on ABCG2. WT, *Abcg2*-null, *Fech*-mut, and *Fech*-mut/*Abcg2*-null mice were kept under the same environment and euthanized at a similar age. (A to C) Serum activities of alanine transaminase (ALT), aspartate transaminase (AST), and alkaline phosphatase (ALP). (D) Serum total bilirubin. (E) PPIX in the liver, analyzed by UPLC-QTOFMS. The data are expressed as means \pm SEM ($n = 4$ per group). *** $P < 0.001$, one-way ANOVA. (F to I) Representative liver sections with H&E staining. Arrows indicate bile plugs. Scale bars, 10 μ m. PV, portal vein; BD, bile duct.

In EPP, PPIX in the liver comes mainly from the bone marrow through the circulatory system, followed to a lesser extent by de novo synthesis in hepatocytes (5, 15). Accumulation of PPIX in the liver causes liver damage that can be life threatening because of liver failure (5, 15). Here, we demonstrated that EPP-associated hepatotoxicity is dependent on ABCG2, which builds up a high level of PPIX in the biliary system and leads to bile duct blockage (Fig. 6A). This is a vicious cycle because ABCG2-mediated bile duct blockage prevents PPIX excretion, resulting in further accumulation of PPIX in the body and thus increases PPIX-mediated toxicities (Fig. 6A). ABCG2

deficiency breaks this vicious cycle of PPIX accumulation caused by FECH deficiency or porphyrinogenic chemicals by decreasing PPIX delivery to the hepatobiliary system and relieving PPIX-mediated bile duct blockage (Fig. 6B). In addition, ABCG2 deficiency retains PPIX in hepatocytes where it can be metabolized to conjugated products to facilitate their excretion (Fig. 6B). These data suggest that ABCG2 is a potential target for the management of EPP-associated hepatotoxicity.

Our work shifts current research paradigms for the roles of ABCG2 in porphyrin homeostasis and toxicities. A previous report

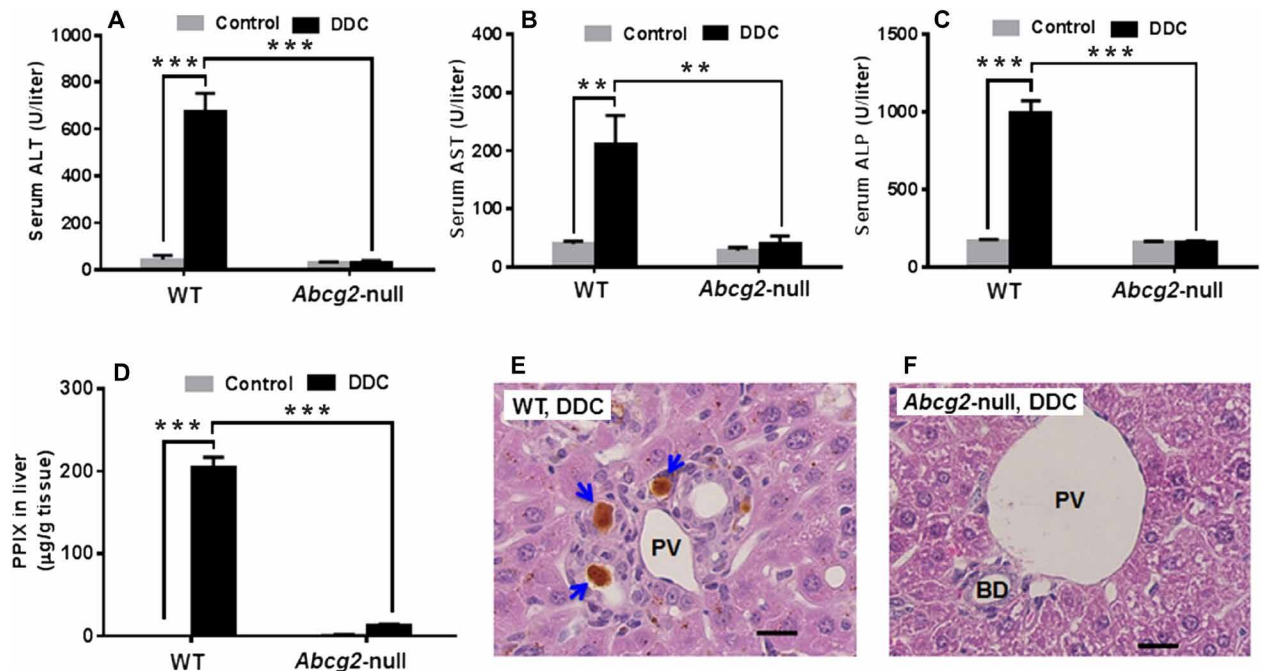


Fig. 3. PPIX accumulation and hepatotoxicity in WT and *Abcg2*-null mice treated with DDC. (A to C) Serum activities of ALT, AST, and ALP. (D) PPIX in the liver, analyzed by UPLC-QTOFMS. All data are expressed as means \pm SEM ($n = 3$ to 4 per group). $**P < 0.01$, $***P < 0.001$, two-way ANOVA. (E and F) Histologic analysis of the liver with H&E staining. Arrows point to bile plugs. Scale bars, 10 μm .

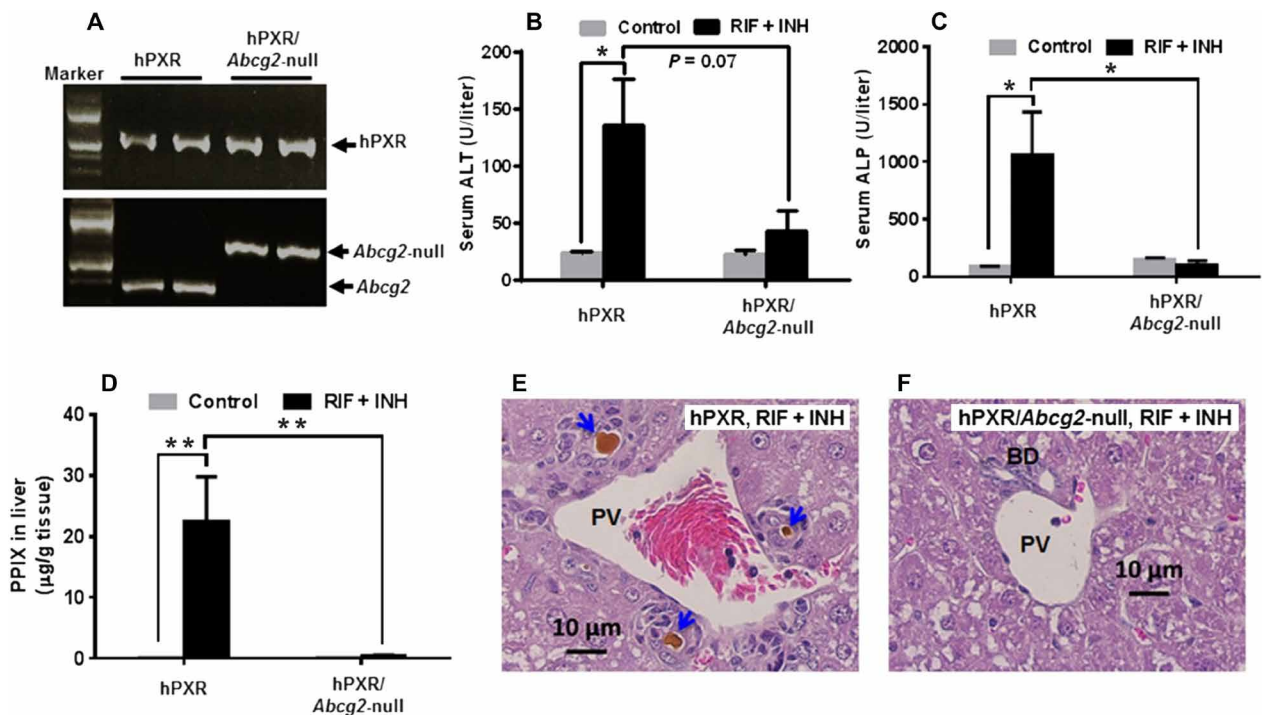


Fig. 4. PPIX accumulation and hepatotoxicity in hPXR and hPXR/*Abcg2*-null mice treated with RIF and INH. (A) Genotyping results of hPXR and hPXR/*Abcg2*-null mice. (B and C) Serum activities of ALT and ALP. (D) PPIX in the liver, analyzed by UPLC-QTOFMS. All data are expressed as means \pm SEM ($n = 3$ to 4 per group). $*P < 0.05$, $**P < 0.01$, two-way ANOVA. (E and F) Histologic analysis of liver with H&E staining. Arrows point to bile plugs.

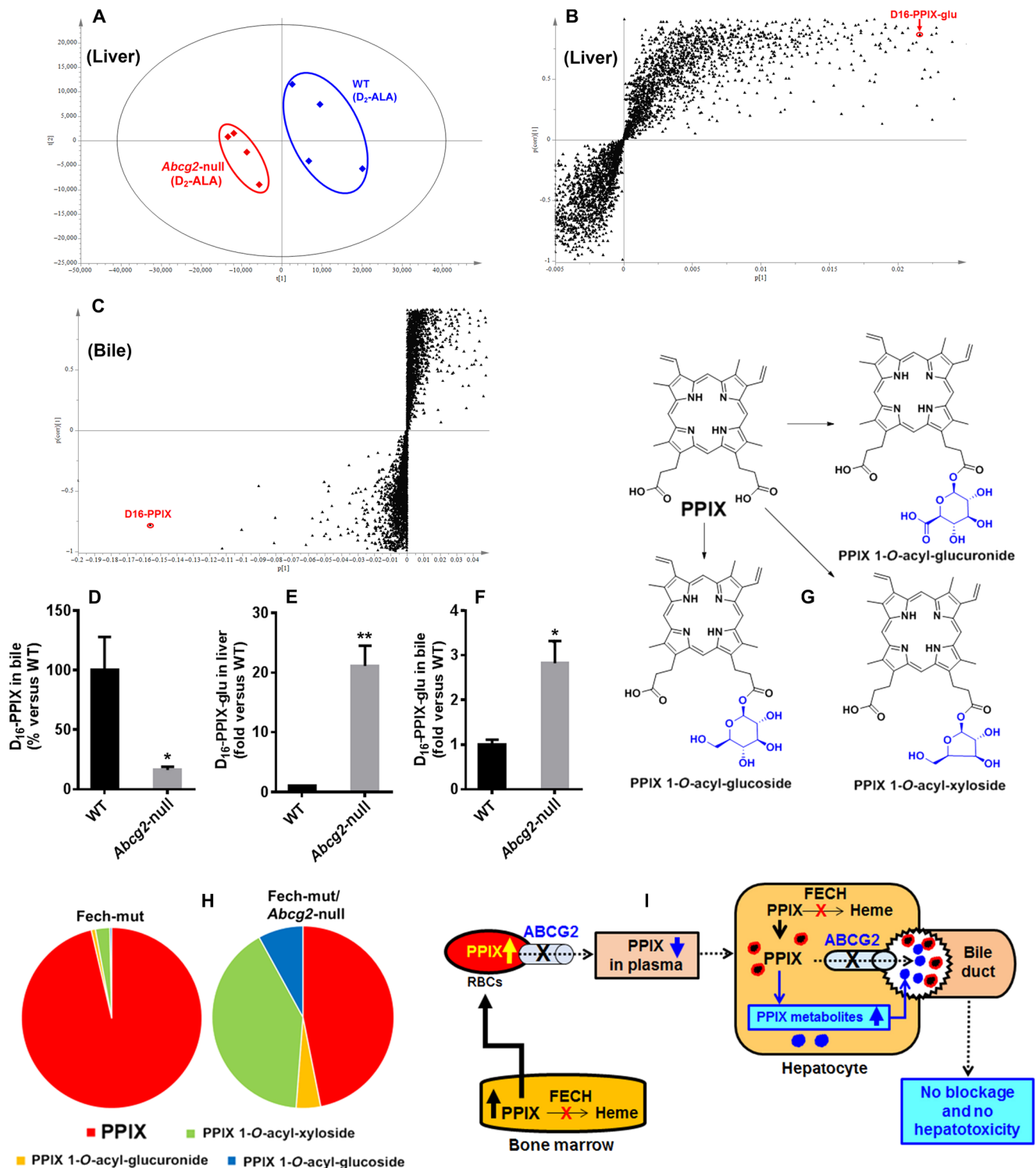


Fig. 5. Deficiency of ABCG2 modulates PPIX distribution, metabolism, and excretion. (A to F) Metabolomic analyses in WT and *Abcg2*-null mice treated with deuterium-labeled aminolevulinic acid (D₂-ALA), a precursor of PPIX. Liver and bile samples were collected at 1 hour after D₂-ALA treatment. (A) Score plots of liver samples generated by principal components analysis. Each point represents a mouse sample. (B and C) S-plots of liver and bile metabolome generated by orthogonal partial least-squares discriminant analysis. Each point represents a metabolite. All metabolites were analyzed by UPLC-QTOFMS. (D) D₁₆-PPIX in the bile. (E and F) D₁₆-protoporphyrin-1-O-acyl-glucuronide (D₁₆-PPIX-glu) in the liver and bile. All the data are expressed as means ± SEM. The data in WT were set as 100% or 1. **P* < 0.05, ***P* < 0.01, two-tailed Student's *t* test. (G) The structures of PPIX and its conjugated metabolites with glucuronic acid, xylose, and glucose. (H) The percentages of PPIX and its conjugated metabolites in the bile of *Fech*-mut and *Fech*-mut/*Abcg2*-null mice. (I) A schematic showing deficiency of ABCG2 abolishes EPP-associated liver injury by modulating PPIX distribution, metabolism, and excretion.

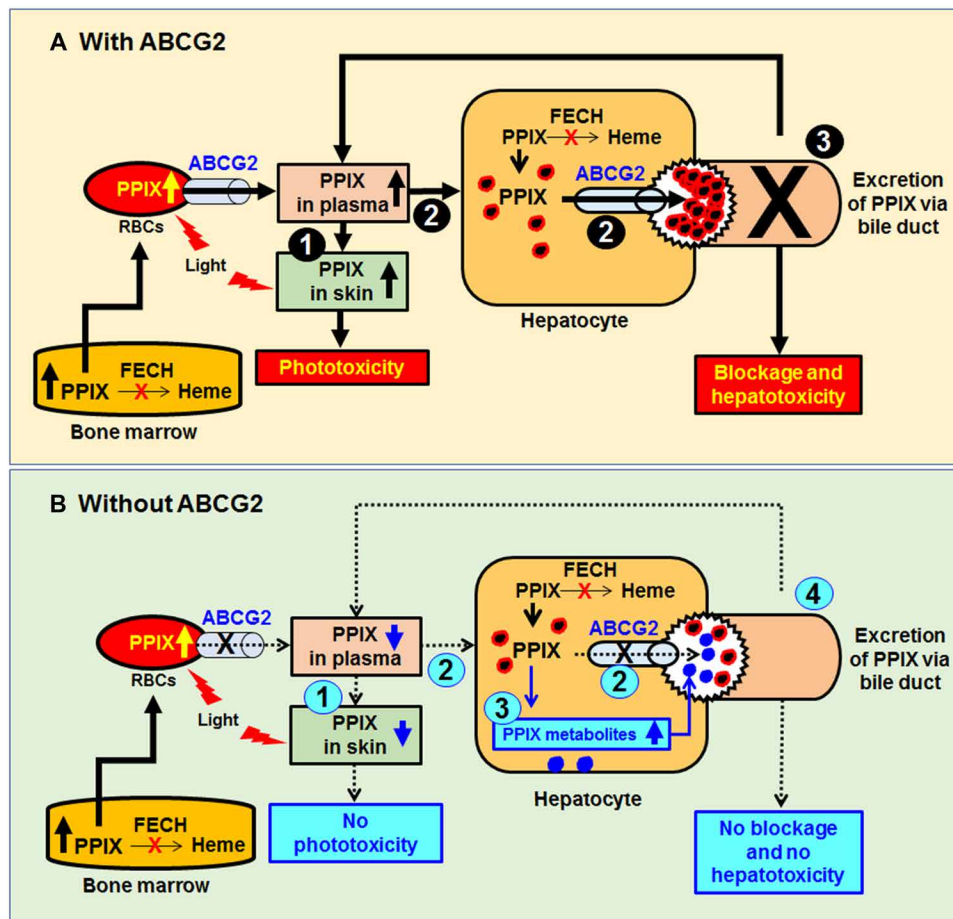


Fig. 6. A summary of the roles of ABCG2 in the pathophysiology of EPP. ABCG2 is expressed in RBCs and hepatocytes. (A) A schematic showing ABCG2 drives phototoxicity and hepatotoxicity in EPP by (1) increasing PPIX distribution to the skin and increasing photosensitivity; (2) increasing PPIX delivery to the hepatobiliary system and causing bile duct blockage and cholestatic liver injury; and (3) ABCG2-dependent bile duct blockage further increases PPIX accumulation in the body, which, in turn, potentiates both phototoxicity and hepatotoxicity. (B) A schematic showing deficiency of ABCG2 abolishes phototoxicity and hepatotoxicity in EPP by (1) decreasing PPIX distribution to the skin and decreasing photosensitivity; (2) decreasing PPIX delivery to the hepatobiliary system and relieving PPIX-mediated bile duct blockage; (3) the retained PPIX in hepatocytes can be further metabolized to conjugated products to facilitate their excretion; and (4) prevention of PPIX-mediated bile duct blockage decreases PPIX accumulation in the body and attenuates both phototoxicity and hepatotoxicity.

showed that *Abcg2*-null mice are sensitive to an exogenous phototoxin, pheophorbide A (PPA), which is an analog of PPIX and a substrate of ABCG2 (24). This phototoxicity model is totally different from EPP, because oral treatment with PPA bypasses ABCG2 in RBCs and PPA is directly delivered to the skin, whereas the distribution of PPIX to the skin in EPP is dependent on ABCG2 in RBCs and deficiency of ABCG2 decreases the distribution of PPIX to the skin. In addition, deficiency of ABCG2 in the intestine increases the bioavailability of PPA by preventing its efflux back into the intestinal lumen. Furthermore, PPA cannot be further metabolized through conjugation pathways because a methyl group already occupies one of the conjugation positions in PPA. Moreover, deficiency of ABCG2 in hepatocytes blocks PPA excretion through the biliary system, and thus, PPA will return to the circulatory system and deposit more in the skin and increase phototoxicity.

Some pertinent questions for dysfunction of ABCG2 in EPP are whether the accumulation of PPIX in RBCs will be safe and what the fate of the high level of PPIX in RBCs is. We analyzed mean corpuscular hemoglobin (MCH) and total hemoglobin (tHb)

in the blood of EPP mouse models and observed decreases of MCH and tHb in *Fech*-mut mice, but not in *Fech*-mut/*Abcg2*-null mice (fig. S8). In addition, *Fech*-mut/*Abcg2*-null mice appear healthy with a normal breeding pattern compared to *Fech*-mut mice with difficulties in breeding. Spleen enlargement has been observed in patients with EPP (31). Deficiency of ABCG2 attenuates EPP-associated spleen enlargement (fig. S9A), although the PPIX level in the spleen of *Fech*-mut/*Abcg2*-null mice was higher than that of *Fech*-mut mice (fig. S9B). These data suggest that PPIX accumulation in RBCs is safe in EPP with ABCG2 deficiency. RBCs have a lifespan of ~120 days; afterward, they are recycled by macrophages in the spleen and liver. Therefore, it is likely that the high level of PPIX in RBCs of *Fech*-mut/*Abcg2*-null mice will end up in the macrophages of the spleen and liver, and this seems protective because a previous study showed that retention of PPIX in Kupffer cells, the resident liver macrophages, attenuates EPP-associated hepatotoxicity (23). Further studies are needed to determine the metabolism and disposition of PPIX in the macrophages of the spleen and liver.

In summary, the current work demonstrated that the transporter ABCG2 is the key mediator in the pathophysiology of EPP, suggesting that ABCG2 is a potential target for EPP therapy. Our findings in EPP can also be applied for managing the toxicities of porphyrinogenic drugs/chemicals and XLP, because they all have a similar biochemical basis to EPP in PPIX accumulation.

MATERIALS AND METHODS

Animal development, characterization, and maintenance

Fech-mut/*Abcg2*-null mice were generated by crossing Fech-mut mice with *Abcg2*-null mice and were backcrossed with Fech-mut mice for at least three generations. *Abcg2*-null mice, originally generated in Schinkel's group (24), were obtained from Taconic Biosciences Inc. (Hudson, NY). Fech-mut mice were purchased from the Jackson Laboratory (Bar Harbor, ME), which were originally developed on the basis of a loss-of-function mutation of FECH (25, 26). Fech-mut/*Abcg2*-null mice were verified by polymerase chain reaction (PCR) genotyping of Fech mutation and mouse *Abcg2*. hPXR/*Abcg2*-null mice were generated by crossing hPXR mice with *Abcg2*-null mice and were backcrossed with hPXR mice for at least three generations. hPXR mice were originally generated by bacterial artificial chromosome transgenesis (32). hPXR/*Abcg2*-null mice were verified by PCR genotyping of human *PXR*, mouse *Pxr*, and mouse *Abcg2*. All mice (2- to 4-month-old, male) were kept under standard 12-hour light/dark cycle. The roles of ABCG2 in PPIX toxicities were determined in paired studies using WT versus *Abcg2*-null, hPXR versus hPXR/*Abcg2*-null, and Fech-mut versus Fech-mut/*Abcg2*-null mice, respectively. The handling of mice was in accordance with study protocols approved by the Institutional Animal Care and Use Committees of University of Pittsburgh and University of Kansas Medical Center.

Animal studies to determine the role of ABCG2 in EPP-associated phototoxicity

WT, *Abcg2*-null, Fech-mut, and Fech-mut/*Abcg2*-null mice were used to determine the role of ABCG2 in EPP-associated phototoxicity. Phototoxicity was examined using a similar approach as described previously (33). In brief, the back skin of mice was shaved and exposed to ultraviolet (UV) light [DULEX, 395 to 410 nm, 294 lumens (lm)/m²] for 30 min each day and continued for 5 days. On the sixth day, all mice were euthanized. The back skin was harvested for histological analysis. Skin samples were also used for measurement of PPIX. In addition, red light (UltraFire, 630 nm, 6164 lm/m²) was used to determine whether the long-wavelength visible radiation can cause phototoxicity in Fech-mut and Fech-mut/*Abcg2*-null mice.

Animal studies to determine the role of ABCG2 in EPP-associated hepatotoxicity

WT, *Abcg2*-null, Fech-mut, and Fech-mut/*Abcg2*-null mice were kept under the same environment and euthanized at a similar age. Liver and blood samples were collected for evaluation of liver damage. Liver, bile, spleen, and blood samples were used for analysis of PPIX and its metabolites.

Animal studies to determine the role of ABCG2 in chemically induced PPIX accumulation and hepatotoxicity

WT and *Abcg2*-null mice were treated with DDC (0.1% in diet) or GSF (2.5% in diet) for 2 weeks. In addition, hPXR and hPXR/*Abcg2*-null mice were treated with RIF (100 mg/kg diet) and INH (400 mg/liter

drinking water) for 4 weeks. After treatment, blood and liver samples were collected for evaluation of liver injury and analysis of PPIX.

Animal studies to determine the role of ABCG2 in modulating PPIX distribution, metabolism, and excretion

WT and *Abcg2*-null mice were treated with D₂-ALA (50 mg/kg, intraperitoneally), a stable isotope-labeled precursor of PPIX. One hour after D₂-ALA treatment, liver and bile samples were collected for metabolomic analysis. In brief, liver and bile samples were analyzed using ultra-performance liquid chromatography coupled with a quadrupole time-of-flight mass spectrometer (UPLC-QTOFMS, Waters Corp, Milford, MA). Centroid and integrated mass chromatographic data were processed by MarkerLynx software (Waters Corp, Milford, MA) to generate a multivariate data matrix. These data were then exported to SIMCA-P+ software (Umetrics, Kinnelon, NJ) for multivariate data analysis. Principal components analysis and orthogonal projection to latent structures discriminant analysis were conducted to represent the major latent variables in the data matrix. The variables that substantially contributed to the discrimination between groups were subjected to structure identification.

Statistics

Data are shown as means ± SEM. Statistical analysis was performed using GraphPad Prism 7.0. One-way or two-way analysis of variance (ANOVA) with Tukey's post hoc tests was used to compare differences among multiple groups. Two-tailed Student's *t* tests were used to compare differences between two groups. A *P* value <0.05 was considered as statistically significant.

SUPPLEMENTARY MATERIALS

Supplementary material for this article is available at <http://advances.sciencemag.org/cgi/content/full/5/9/eaaw6127/DC1>

Supplementary Materials and Methods

Fig. S1. Histology, oxidative stress, and inflammation in the skin of WT, *Abcg2*-null, Fech-mut, and Fech-mut/*Abcg2*-null mice after the exposure to UV light (395 to 410 nm).

Fig. S2. Gross appearance of Fech-mut and Fech-mut/*Abcg2*-null mice before and after exposure to red light (630 nm).

Fig. S3. Fluorescence of liver samples from WT, *Abcg2*-null, Fech-mut, and Fech-mut/*Abcg2*-null mice.

Fig. S4. Evaluation of liver fibrosis in WT, *Abcg2*-null, Fech-mut, and Fech-mut/*Abcg2*-null mice.

Fig. S5. ABCG2 deficiency abolishes GSF-induced PPIX accumulation and hepatotoxicity.

Fig. S6. Effects of ABCG2 deficiency on the expression of efflux transporters in the liver.

Fig. S7. Identification of PPIX-glu.

Fig. S8. Hematological analysis of blood samples from WT, *Abcg2*-null, Fech-mut, and Fech-mut/*Abcg2*-null mice.

Fig. S9. The ratios of spleen to body weight and PPIX levels in the spleen of WT, *Abcg2*-null, Fech-mut, and Fech-mut/*Abcg2*-null mice.

Table S1. Primers for quantitative PCR analysis.

REFERENCES AND NOTES

- H. L. Bonkovsky, J. T. Guo, W. Hou, T. Li, T. Narang, M. Thapar, Porphyrin and heme metabolism and the porphyrias. *Compr. Physiol.* **3**, 365–401 (2013).
- American Porphyria Foundation (APF, 2014); <http://www.porphyrifoundation.com/about-porphyrin/types-of-porphyrin/EPP>.
- D. M. Becker, J. D. Viljoen, J. Katz, S. Kramer, Reduced ferrochelatase activity: A defect common to porphyria variegata and protoporphyria. *Br. J. Haematol.* **36**, 171–179 (1977).
- S. Kramer, J. D. Viljoen, Erythropoietic protoporphyria: Evidence that it is due to a variant ferrochelatase. *Int. J. Biochem.* **12**, 925–930 (1980).
- M. Balwani, H. Naik, K. E. Anderson, D. M. Bissell, J. Bloomer, H. L. Bonkovsky, J. D. Phillips, J. R. Overbey, B. Wang, A. K. Singal, L. U. Liu, R. J. Desnick, Clinical, biochemical, and genetic characterization of North American patients with erythropoietic protoporphyria and X-linked protoporphyria. *JAMA Dermatol.* **153**, 789–796 (2017).
- S. D. Whatley, S. Ducamp, L. Gouya, B. Grandchamp, C. Beaumont, M. N. Badminton, G. H. Elder, S. A. Holme, A. V. Anstey, M. Parker, A. V. Corrigan, P. N. Meissner, R. J. Hift, J. T. Marsden, Y. Ma, G. Mieli-Vergani, J. C. Deybach, H. Puy, C-terminal deletions

- in the ALAS2 gene lead to gain of function and cause X-linked dominant protoporphyria without anemia or iron overload. *Am. J. Hum. Genet.* **83**, 408–414 (2008).
7. F. Li, J. Lu, J. Cheng, L. Wang, T. Matsubara, I. L. Csanaky, C. D. Klaassen, F. J. Gonzalez, X. Ma, Human PXR modulates hepatotoxicity associated with rifampicin and isoniazid co-therapy. *Nat. Med.* **19**, 418–420 (2013).
 8. A. G. Smith, F. De Matteis, Drugs and the hepatic porphyrias. *Clin. Haematol.* **9**, 399–425 (1980).
 9. R. J. Hift, S. Thunell, A. Brun, Drugs in porphyria: From observation to a modern algorithm-based system for the prediction of porphyrogenicity. *Pharmacol. Ther.* **132**, 158–169 (2011).
 10. G. S. Marks, D. T. Zelt, S. P. Cole, Alterations in the heme biosynthetic pathway as an index of exposure to toxins. *Can. J. Physiol. Pharmacol.* **60**, 1017–1026 (1982).
 11. A. Schauder, A. Avital, Z. Malik, Regulation and gene expression of heme synthesis under heavy metal exposure—Review. *J. Environ. Pathol. Toxicol. Oncol.* **29**, 137–158 (2010).
 12. T. R. Tephly, A. H. Gibbs, F. De Matteis, Studies on the mechanism of experimental porphyria produced by 3,5-dihydroxycarbonyl-1,4-dihydrocollidine. Role of a porphyrin-like inhibitor of protohaem ferro-lyase. *Biochem. J.* **180**, 241–244 (1979).
 13. M. B. Poh-Fitzpatrick, A. A. Lamola, Comparative study of protoporphyrins in erythropoietic protoporphyria and griseofulvin-induced murine protoporphyria: Binding affinities, distribution, and fluorescence spectra in various blood fractions. *J. Clin. Invest.* **60**, 380–389 (1977).
 14. M. Lecha, H. Puy, J.-C. Deybach, Erythropoietic protoporphyria. *Orphanet J. Rare Dis.* **4**, 19 (2009).
 15. H. Puy, L. Gouya, J.-C. Deybach, Porphyrias. *Lancet* **375**, 924–937 (2010).
 16. E. I. Minder, X. Schneider-Yin, J. Steurer, L. M. Bachmann, A systematic review of treatment options for dermal photosensitivity in erythropoietic protoporphyria. *Cell. Mol. Biol.* **55**, 84–97 (2009).
 17. J. G. Langendonk, M. Balwani, K. E. Anderson, H. L. Bonkovsky, A. V. Anstey, D. M. Bissell, J. Bloomer, C. Edwards, N. J. Neumann, C. Parker, J. D. Phillips, H. W. Lim, I. Hamzavi, J. C. Deybach, R. Kauppinen, L. E. Rhodes, J. Frank, G. M. Murphy, F. P. J. Karstens, E. J. G. Sijbrands, F. W. M. de Rooij, M. Lebowohl, H. Naik, C. R. Goding, J. H. P. Wilson, R. J. Desnick, Afamelanotide for erythropoietic protoporphyria. *N. Engl. J. Med.* **373**, 48–59 (2015).
 18. Y. Fukuda, P. L. Cheong, J. Lynch, C. Brighton, S. Frase, V. Kargas, E. Rampersaud, Y. Wang, V. G. Sankaran, B. Yu, P. A. Ney, M. J. Weiss, P. Vogel, P. J. Bond, R. C. Ford, R. J. Trent, J. D. Schuetz, The severity of hereditary porphyria is modulated by the porphyrin exporter and Lan antigen ABCB6. *Nat. Commun.* **7**, 12353 (2016).
 19. A. V. Anstey, R. J. Hift, Liver disease in erythropoietic protoporphyria: Insights and implications for management. *Gut* **56**, 1009–1018 (2007).
 20. B. M. McGuire, H. L. Bonkovsky, R. L. Carithers Jr., R. T. Chung, L. I. Goldstein, J. R. Lake, A. S. Lok, C. J. Potter, E. Rand, M. D. Voigt, P. R. Davis, J. R. Bloomer, Liver transplantation for erythropoietic protoporphyria liver disease. *Liver Transpl.* **11**, 1590–1596 (2005).
 21. S. Zhou, Y. Zong, P. A. Ney, G. Nair, C. F. Stewart, B. P. Sorrentino, Increased expression of the Abcg2 transporter during erythroid maturation plays a role in decreasing cellular protoporphyrin IX levels. *Blood* **105**, 2571–2576 (2005).
 22. S. Sandberg, A. Brun, Light-induced protoporphyrin release from erythrocytes in erythropoietic protoporphyria. *J. Clin. Invest.* **70**, 693–698 (1982).
 23. S. Youmi, M. Abitbol, D. Rainteau, Z. Karim, F. Bernex, V. Oustric, S. Millot, P. Lettéron, N. Heming, L. Guillmot, X. Montagutelli, G. Berdeaux, L. Gouya, R. Poupon, J. C. Deybach, C. Beaumont, H. Puy, Protoporphyrin retention in hepatocytes and Kupffer cells prevents sclerosing cholangitis in erythropoietic protoporphyria mouse model. *Gastroenterology* **141**, 1509–1519 (2011).
 24. J. W. Jonker, M. Buitelaar, E. Wagenaar, M. A. van der Valk, G. L. Scheffer, R. J. Scheper, T. Plösch, F. Kuipers, R. P. J. O. Efferink, H. Rosing, J. H. Beijnen, A. H. Schinkel, The breast cancer resistance protein protects against a major chlorophyll-derived dietary phototoxin and protoporphyria. *Proc. Natl. Acad. Sci. U.S.A.* **99**, 15649–15654 (2002).
 25. S. Tutois, X. Montagutelli, V. Da Silva, H. Jouault, P. Rouyer-Fessard, K. Leroy-Viard, J. L. Guénet, Y. Nordmann, Y. Beuzard, J. C. Deybach, Erythropoietic protoporphyria in the house mouse. A recessive inherited ferrochelatase deficiency with anemia, photosensitivity, and liver disease. *J. Clin. Invest.* **88**, 1730–1736 (1991).
 26. S. Boulechfar, J. Lamoril, X. Montagutelli, J. L. Guenet, J. C. Deybach, Y. Nordmann, H. Dailey, B. Grandchamp, H. de Verneuil, Ferrochelatase structural mutant (Fechm1Pas) in the house mouse. *Genomics* **16**, 645–648 (1993).
 27. C. K. Lim, M. A. Razzaque, J. Luo, P. B. Farmer, Isolation and characterization of protoporphyrin glycoconjugates from rat Harderian gland by HPLC, capillary electrophoresis and HPLC/electrospray ionization MS. *Biochem. J.* **347**, 757–761 (2000).
 28. C. Xu, C. Y.-t. Li, A.-n. T. Kong, Induction of phase I, II and III drug metabolism/transport by xenobiotics. *Arch. Pharm. Res.* **28**, 249–268 (2005).
 29. H. Baart de la Faille, J. C. Bijlmer-est, J. van Hattum, J. Koningsberger, L. H. Rademakers, H. van Weelden, Erythropoietic protoporphyria: Clinical aspects with emphasis on the skin. *Curr. Probl. Dermatol.* **20**, 123–134 (1991).
 30. M. Balwani, R. J. Desnick, The porphyrias: Advances in diagnosis and treatment. *Hematology Am. Soc. Hematol. Educ. Program* **2012**, 19–27 (2012).
 31. N. S. Key, J. M. Rank, D. Freese, J. R. Bloomer, D. E. Hammerschmidt, Hemolytic anemia in protoporphyria: Possible precipitating role of liver failure and photic stress. *Am. J. Hematol.* **39**, 202–207 (1992).
 32. X. Ma, Y. Shah, C. Cheung, G. L. Guo, L. Feigenbaum, K. W. Krausz, J. R. Idle, F. J. Gonzalez, The pregnane X receptor gene-humanized mouse: A model for investigating drug–drug interactions mediated by cytochromes P450 3A. *Drug Metab. Dispos.* **35**, 194–200 (2007).
 33. R. Pawliuk, R. Tighe, R. J. Wise, M. M. Mathews-Roth, P. Leboulch, Prevention of murine erythropoietic protoporphyria-associated skin photosensitivity and liver disease by dermal and hepatic ferrochelatase. *J. Invest. Dermatol.* **124**, 256–262 (2005).
- Acknowledgments:** We thank S. Ofori-Acquah's laboratory for the blood test. We also thank J. Maddigan for reviewing and editing the manuscript. Photo credit: Pengcheng Wang (Fig. 1B) and Jing Chen (fig. S2), University of Pittsburgh. **Funding:** This work was supported in part by the National Institute of Diabetes and Digestive and Kidney Diseases (R01DK090305) and the National Institute of Allergy and Infectious Diseases (R01AI131983). **Author contributions:** X.M., P.W., and M.S. conceived the project and wrote the manuscript. P.W., M.S., J.L., A.I.S., J.Z., J.C., K.L., and X.M. performed the experiments. W.X., F.J.G., C.D.K., and X.M. contributed to the new reagents, analytic tools, and animal models. X.M., K.E.A., W.X., F.J.G., and C.D.K. contributed to the scientific discussion and experimental design. **Competing interests:** X.M., J.Z., and J.L. are inventors on a patent application related to this work filed with the United States Patent and Trademark Office (no. 62/850,061, filed: 20 May 2019). The authors declare no other competing interests. **Data and materials availability:** All data needed to evaluate the conclusions in the paper are present in the paper and/or the Supplementary Materials. Additional data related to this paper may be requested from the authors.
- Submitted 9 January 2019
 Accepted 23 August 2019
 Published 18 September 2019
 10.1126/sciadv.aaw6127
- Citation:** P. Wang, M. Sachar, J. Lu, A. I. Shehu, J. Zhu, J. Chen, K. Liu, K. E. Anderson, W. Xie, F. J. Gonzalez, C. D. Klaassen, X. Ma, The essential role of the transporter ABCG2 in the pathophysiology of erythropoietic protoporphyria. *Sci. Adv.* **5**, eaaw6127 (2019).